Well-seismic bandwidth and time-lapse seismic characterization related to CO_2 injection and fluid substitution: physical considerations

Yinbin Liu and Don C. Lawton, CREWES, Department of Geology and Geophysics, University of Calgary*

Summary

Reservoirs are commonly heterogeneous. Injection of CO_2 (or other fluids) related to enhanced oil recovery (EOR) operations may cause strong lateral and depth-dependent changes of heterogeneity both within the reservoir and in the surrounding formations. A seismic signal propagating through the reservoir and the surrounding formations before and after the injection undergoes different velocity dispersion and amplitude attenuation, which result in time shifts and waveform distortion. This paper discusses the physical aspects of well log integration with seismic and time-lapse seismic characterization based on a thinly layered model (1D heterogeneity). The results show that discrete layering and interval multiple reflections (or scattering) within sedimentary sequences have a significant influence on synthetic seismograms. The velocity and density perturbations inside and outside the reservoir will mainly result in the time-lapse amplitude anomaly at the top of the reservoir and the local coda wave distortion from near the top of the reservoir to the strong basal reflection below the reservoir (BBR). The distortion of the coda wave is highly dependent on the magnitudes of medium perturbations. Large perturbations may cause time a sag for the basal reflection as well as later events, which mainly include primary reflections. Those results have important implications for time-lapse seismic monitoring.

Introduction

Sonic logs and seismic surveys measure the acoustic responses of the earth with different resolutions. Sonic logs can usually identify individual sedimentary layers at tens of centimetres in thickness (borehole scale), and a seismic reflector is usually the overall response of many sedimentary layers at a scale of tens of meters. Physically speaking, seismic and sonic logs should be thoroughly integrated. There is a need to physically fill the gap between sonic bandwidth and seismic bandwidth so as to identify small-scale reservoir and to monitor reservoir characterization from seismic data.

Production of hydrocarbons and injection of CO_2 (or other fluids) related to EOR operations will cause changes in sonic velocity and density both inside the reservoir (changes of both fluid properties and stress) and outside the reservoir (change of stress). These changes may be observed on time-lapse seismic data. For example, we can observe the waveform distortion in the reservoir section and "pushdown" effect or time sag for reflections below the reservoir (e.g., Li, 2003; Calvert, 2005). However, the corresponding relationships between the changes of time-lapse seismic data and fluid saturation and distribution have not been established. The multiple scattering of seismic wave within heterogeneous reservoirs remains poorly understood.

Seismic wave propagation and scattering in strong 1D heterogeneity can be modeled by a propagator matrix approach (e.g., Liu and Schmitt, 2000). In this paper we first study frequency-dependent seismic reflections for a blocked wedge model. Then the influence of interval multiple scattering on seismic reflection is analyzed. Acoustic velocity associated with rock deformation processes is discussed. Finally, time-lapse seismic characterization is studied by blocking the reservoir and the surrounding formations into many thin layers with depth-dependent velocity and density perturbations.

Well-seismic bandwidth

Frequency-dependent seismic reflections Understanding for scale-dependent velocity dispersion and amplitude attenuation of seismic waves (well-seismic bandwidth) within sedimentary sequences is a key issue for subtle reservoir characterizations. Figure 1 (brown line) is a wedge model (Hilterman, 2001) with velocity changes from 2250 m/s to 4500 m/s and density changes from 2.393 g/cm^3 to 2.8716 g/cm^3 over a 200 m depth. The model can be approximately blocked into 20 transitional layers, each 10 m thick (the velocity increases in a step of 112.5 m/s and the density increases in a step of 0.02393 g/cm^3). A propagator matrix method is employed to study the reflection characterization. Figure 1 (blue lines) shows the calculated normal seismic reflections for a zero-phase Ricker wavelet source with dominant frequencies from 20 Hz to 400 Hz. The corresponding λ/d changes are from 8.5 to 0.4. The time triggers are the starting points of the first arrivals (green line). The waveforms show polarity reversals because the reflections are from high to low impedance layers. It can be seen that seismic reflections are the cumulative effects of the transitional layers, and main waveform distortion is from a strong and abrupt contrast of acoustic impedance which is on the top boundary. It is difficult to identify the reflections for the individual transitional layers for low frequency incident waves

($\lambda/d >$ about 2). However, the coda waves produced by multiple reflections or scattering for high frequency incident waves (about $2 > \lambda/d >$ about 0.8) can be clearly seen. As λ/d decreases further ($\lambda/d <$ about 0.8), the later arriving reflections can be identified.

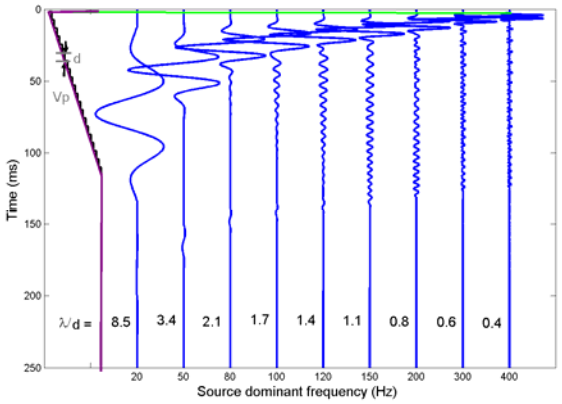

Figure 1: Reflection synthetics of a blocked wedge model for different frequency Ricker wavelet sources.

Primary and multiples Figure 2a shows sonic and density logs from a well in central Alberta. The changes of density and velocity are large in the overburden and are slightly larger in the reservoir section than those in the surrounding formations. In this study we block the logs from 308 m to 2221 m into about 1350 layers. Figures 2b and 2c show the blocked density and velocity logs and the corresponding perturbations inside and outside the reservoir caused by CO_2 injection. Figure 3 shows the normal reflection synthetic seismograms for a 50 Hz zero-phase Ricker wavelet source before medium perturbations. The blue and red lines stand for the results from primary reflections (conventional convolution model) and multiple reflections (propagator matrix, which includes both primary and multiples), respectively. It can be seen that there is a large difference between synthetic seismograms when multiples are included. The longer the propagation time or distance, the larger the waveform distortion is. The amplitude difference at about 1300 ms is up to about 500%. This is because a long propagation time or traveling distance will include more multiple waves. The multiple scattering in a strong 1D heterogeneity results in large waveform distortion (amplitude, frequency, and phase or time).

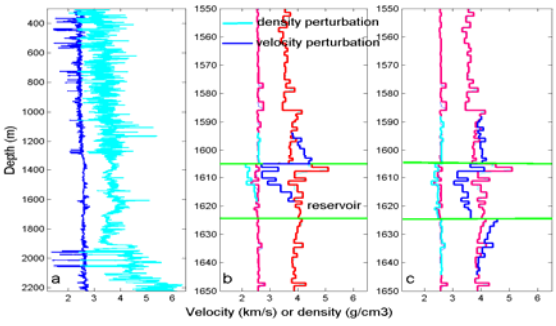

Figure 2: Density and sonic logs and density and velocity perturbations inside and outside the reservoir.

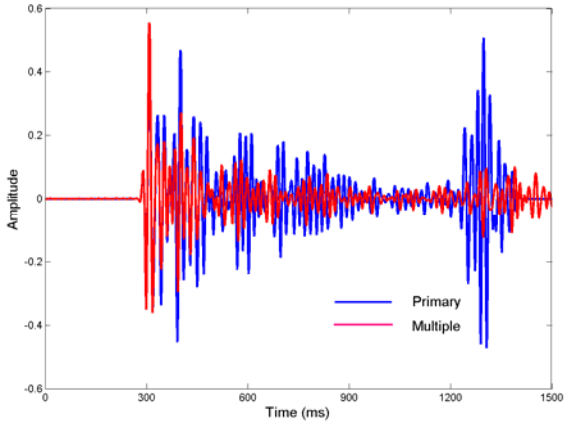

Figure 3: Primary (blue) and multiple (red) synthetic seismograms before medium perturbations.

Acoustic velocity in rock deformation processes

Rock deformation During production of hydrocarbons and injection of CO_2, the reservoirs and the surrounding rocks undergo both elastic and inelastic deformation caused by pore fluid pressure changes. These include elasticity, dilatancy, pore collapse, and normal consolidation (Scott et al., 1998). As strain increases, the sonic velocity tends to increase in elastic region, decrease in dilatancy and pore collapse regions, and increase in the normal consolidation region. Mechanical rock damage will change the elastic moduli of the skeletons of porous rocks (inelasticity). Pore collapse may dramatically decrease propagation velocity and increase amplitude attenuation. For example, the sonic velocity of unconsolidated sands may be much less than that of the saturated fluid (Kvamme et al., 1997). This is because the acoustic property of an unconsolidated fluid/solid two-phase medium is dominated by the compressibility of a fluid and the density of a solid. Gassmann's equation and Biot's theory, based on linear elasticity assumptions (the shear moduli for dry and saturated rocks are the same), usually underestimate the velocity of porous medium and cannot well explain the observed time-lapse seismic data (Ng et al., 2005).

CO_2 injection model During injection into the reservoir in Figure 2, CO_2 tends to move up and first substitutes or mixes with the original pore fluids near the top of the

reservoir (or also leaks occasionally into the formations above the reservoir), and causes the changes of pore fluid saturation within reservoir and stress changes both inside reservoir (vertical elongation) and the surrounding rocks (vertical contraction). The changes in velocity and density will tend to decrease with depth inside the reservoir. The thickness of the reservoir sand in the studied area is about 18.5 m (depth from about 1605 m to 1623.5 m), which is blocked into 14 thin layers in Figures 2b and 2c (the thickness of each blocked layer is much less than the seismic wavelength). Total thickness of the perturbations within the reservoir is basically the same as that of the surrounding formations. In this study, we build three kinds of models to simulate depth-dependent velocity and density perturbations: (1) perturbations only inside the reservoir (Figure 2b); (2) perturbations both inside and above the reservoir (Figure 2b); (3) perturbations both inside and outside the reservoir (Figure 2c). The depth-dependent perturbations can be incorporated into a layered model by blocking the reservoir and the surrounding rocks into many thin layers (1D heterogeneity). The large change of heterogeneity near the top of the reservoir produced by CO_2 injection is simulated by the thin layers with large perturbations. The thickness changes caused by reservoir compaction or elongation and surface subsidence or rising (Sen and Settari, 2005) are ignored in this study.

Time-lapse synthetic seismic characterization

Time-lapse seismic anomalies are the responses of velocity and density perturbations inside the reservoir and the surrounding formations (Lines et al., 2003). Figure 4 shows the influence of depth-dependent velocity and density perturbations both inside and above the reservoir on seismic reflections for a 50 Hz zero-phase Ricker wavelet. For each injected CO_2 thickness, the depth-dependent velocity and density perturbations are from -40% to 0% and from -15% to 0%, and the corresponding perturbations above the reservoir are from 20% to 0% and from 1% to 0%, respectively. Figure 2b shows that the velocity and density perturbations inside the reservoir (12.0 m) and above the reservoir (12.0 m). In Figure 4 the red lines show a seismic reflection before medium perturbations. The blue and green lines are seismic reflections from only the reservoir perturbations and from both inside and above the reservoir perturbations, respectively.

Figure 5 shows the influence of velocity and density perturbations both inside and outside the reservoir on seismic reflections (entire reservoir perturbations). The velocity and density perturbations outside the reservoir are from 10% to 0% and from 1% to 0%, respectively, and the velocity and density perturbations inside the reservoir are given in 5 values: (1) -10% velocity perturbation and -5% density perturbation for the entire reservoir (see Figure 2c); (2) the perturbation changes from the top to the bottom of the reservoir are from -20% to -10% for the velocities and -5% to -2.5% for the densities; (3) is the same as (2) except from -30% to -10% for the velocities and -10% to -5% for the densities; (4) is the same as (3) except from -30% to -20% for the velocities; (5) is the same as (3) except from -40% to -20% for the velocities. The red lines show a seismic reflection before medium perturbation and the blue lines after different velocity and density perturbations. Figures 4 and 5 show that the top reservoir reflection is at about 1060 ms and the strong base reflection below the reservoir (BBR, Viking formation) is at about 1280 ms, the latter is a strong seismic reflection because of strong impedance contrasts for this event.

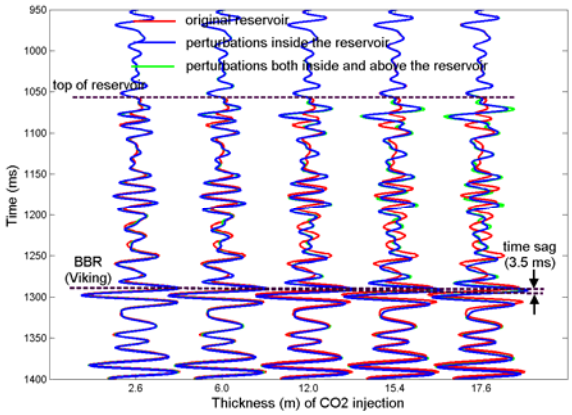

Figure 4: Influence of velocity and density perturbations both inside and above the reservoir on seismic reflections.

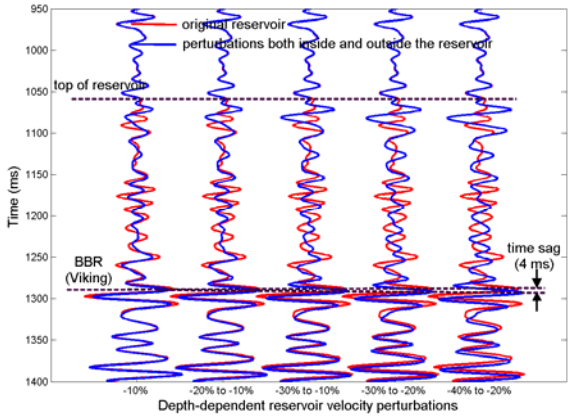

Figure 5: Influence of velocity and density perturbations both inside and outside the reservoir on seismic reflections.

The modeling results suggest that the influences of velocity and density perturbations outside the reservoir are small for travel time and may be significant for the reflection strengths on the top of the reservoir (Figure 4) and the BBR

(Figure 5). This is because the depth-dependent velocity and density perturbations produce the cumulative effects on the boundaries of the top and bottom of the reservoir as discussed in Figure 1. It can be seen that the velocity and density changes of the reservoir and the surrounding formations will result in time-lapse amplitude anomaly on the top of the reservoir, waveform distortion from the top of the reservoir to the BBR reflection, and both time sag and amplitude anomaly for the BBR reflection or later events (the time sags from the left to the right in Figures 4 and 5 are from about 1 ms to 4 ms). The overall differences of time-lapse seismic reflections increase with increasing medium perturbations (amount of CO_2 injection). The time-lapse amplitude anomaly may be very large for the reflection on the top of the reservoir (the anomaly can go up to 100% or more). The multiple scattering waves caused by CO_2 injection are usually weaker than a BBR primary reflection. Therefore, the BBR reflection mainly includes primary reflections and undergoes small waveform distortion after medium perturbations. However, the BBR reflection and later events, which travel through the reservoir twice, may cause time sag or "pushdown" effect and amplitude anomaly as seen in Figures 4 and 5.

The waveform distortion caused by the perturbations inside and outside the reservoir mainly takes place in the section from near the top of the reservoir to the BBR reflection. This kind of phenomenon may be related to wave localization in strong heterogeneity (Sheng, 1995), we call it time-lapse "local coda wave". The distortion of the local coda wave is highly dependent on the magnitudes of medium perturbations. A small amount of CO_2 injection or a thin injected CO_2 layer will mainly cause a time-lapse amplitude anomaly while a large amount of CO_2 injection or a thick injected CO_2 layer with large reservoir perturbations will also cause the coda wave distortion and the time sag for the BBR reflection or later events.

Discussion

Production of hydrocarbons and injection of CO_2 (or other fluids) may cause rock elasticity and inelasticity deformation and result in changes in velocity and attenuation. However, the relationships between velocity and attenuation and rock deformation are not well established. This means that further work is needed for porous medium deformation model. Time-lapse seismic survey is primarily interested in monitoring the changes of reservoir fluids, rather than in detecting the detailed distributions of reservoir fluids. In this study, changes of the local coda wave from near the top of the reservoir to the BBR reflection is an amplified seismic response of the reservoir and the surrounding formation perturbations because the wave has been scattered many times before leaving the reservoir (changes of localized wave or localization). Snieder and his research fellows in Colorado School of Mines have developed a technique called "coda wave interferometry" to extract the medium perturbation information from the changes in the multiple scattered waves. "Coda wave interferometry" or "local coda wave" spectroscopy is probably most suitable technique for seismic reservoir monitoring. Seismic physical analyses (scale-dependent and angle-dependent multiple scattering or anisotropic Q) for reflections from the top of the reservoir, the local coda wave, and the BBR reflection or later events, may possibly provide useful clues for the determination of distributions and levels of CO_2 injection.

Acknowledgments

The authors thank for the support of the CREWES project in the Department of Geology and Geophysics, University of Calgary, and from NSERC. YBL appreciates the suggestions and discussions with Gary F. Margrave and John Zhang.

References

Calvert, R., 2005, Insights and Methods for 4D Reservoir Monitoring and Characterization: 2005 SEG/EAGE Distinguished Instructor Short Course.

Hilterman, F. J., 2001, Seismic Amplitude Interpretation: 2001 SEG/EAGE Distinguished Instructor Short Course.

Kvamme, L. B., Holt, R. M., and Nes, O. M.,1997, Acoustic velocities in unconsolidated sands: EAGE 59th conference and technical exhibition, FO30.

Li, G., 2003, Fractured reservoir modeling from seismic to simulator: A reality: The Leading Edge, **22**, 684-695.

Lines, L. R., Zou, Y., and Embleton, J., 2003, Reservoir characterization and Heavy oil production: CSEG Recorder, 26, 26-29.

Liu, Y. and Schmitt, D. R., 2000, Quantitative analysis of thin layer effects: Transmission coefficients and seismograms: **70**th Ann. Internat. Mtg. Soc. Expl. Geophys., Expanded Abstracts, 2464-2467.

Ng, H. T., Bentley, L. R., Krebes, E. S., 2005, Monitoring fluid injection in a carbonate pool using time-lapse analysis: Rainbow Lake case study: The Leading Edge, 22,530-534.

Scott Jr., T. E., Zaman, M.M., and Roegiers, J. C., 1998, Acoustic-velocity signatures associated with rock-deformation processes: JPT (June, 1998),70-74.

Sen, V., and Settari, A., 2005, Coupled geomechanical and flow modeling of compacting reservoirs: The Leading Edge, **24**, 1284--1286.

Sheng, P., 1995, Introduction to wave scattering, localization, and mesoscopic phenomena: Academic Press, San Diego.